ISSN: 0095-8972 (Print) 1029-0389 (Online) Journal homepage: <https://www.tandfonline.com/loi/gcoo20>


# Hydrates $[\text{Na}_2(\text{H}_2\text{O})_x](2\text{-thiobarbiturate})_2$ ( $x = 3, 4, 5$ ): crystal structure, spectroscopic and thermal properties

Nicolay N. Golovnev, Maxim S. Molokeyev, Irina V. Sterkhova, Victor V. Atuchin & Maxim Y. Sidorenko


To cite this article: Nicolay N. Golovnev, Maxim S. Molokeyev, Irina V. Sterkhova, Victor V. Atuchin & Maxim Y. Sidorenko (2016) Hydrates  $[\text{Na}_2(\text{H}_2\text{O})_x](2\text{-thiobarbiturate})_2$  ( $x = 3, 4, 5$ ): crystal structure, spectroscopic and thermal properties, Journal of Coordination Chemistry, 69:21, 3219-3230, DOI: [10.1080/00958972.2016.1228914](https://doi.org/10.1080/00958972.2016.1228914)

To link to this article: <https://doi.org/10.1080/00958972.2016.1228914>

 View supplementary material 



 Accepted author version posted online: 25 Aug 2016.  
Published online: 06 Sep 2016.

 Submit your article to this journal 

 Article views: 102

 View related articles 

 View Crossmark data 

 Citing articles: 5 View citing articles 

# Hydrates $[\text{Na}_2(\text{H}_2\text{O})_x](2\text{-thiobarbiturate})_2$ ( $x = 3, 4, 5$ ): crystal structure, spectroscopic and thermal properties

Nicolay N. Golovnev<sup>a</sup>, Maxim S. Molokeev<sup>b,c</sup>, Irina V. Sterkhova<sup>d</sup>, Victor V. Atuchin<sup>e,f,g</sup> and Maxim Y. Sidorenko<sup>a</sup>

<sup>a</sup>Department of Chemistry, Siberian Federal University, Krasnoyarsk, Russia; <sup>b</sup>Laboratory of Crystal Physics, Kirensky Institute of Physics, Krasnoyarsk, Russia; <sup>c</sup>Department of Physics, Far Eastern State Transport University, Khabarovsk, Russia; <sup>d</sup>Laboratory of Physical Chemistry, Irkutsk Favorsky Institute of Chemistry, Irkutsk, Russia; <sup>e</sup>Laboratory of Optical Materials and Structures, Institute of Semiconductor Physics, Novosibirsk, Russia; <sup>f</sup>Functional Electronics Laboratory, Tomsk State University, Tomsk, Russia; <sup>g</sup>Laboratory of Semiconductor and Dielectric Materials, Novosibirsk State University, Novosibirsk, Russia

## ABSTRACT

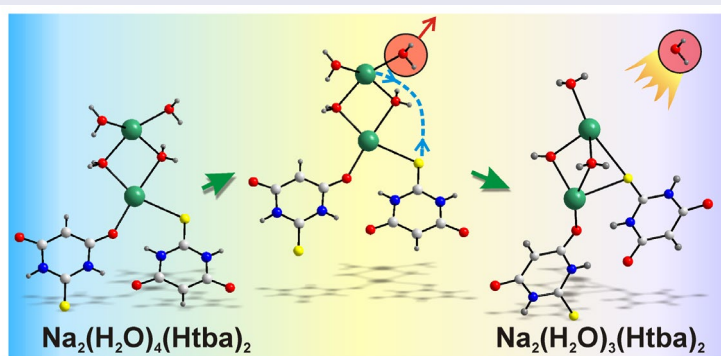
The hydrates  $[\text{Na}_2(\text{H}_2\text{O})_3(\text{Htba})_2]$  (**1**) and  $[\text{Na}_2(\text{H}_2\text{O})_4(\text{Htba})_2]$  (**2**), where H<sub>2</sub>tba is 2-thiobarbituric acid, were obtained under different thermal conditions from aqueous solutions and were structurally characterized. The molecular and supramolecular structures were compared to the known structure of  $[\text{Na}_2(\text{H}_2\text{O})_5(\text{Htba})_2]$  (**3**). In polymeric **1–3**, the Htba<sup>−</sup> ions are linked to Na<sup>+</sup> through O and S forming octahedra. The decrease of the number of coordination water molecules led to an increase of the total number of bridge ligands ( $\mu_2\text{-H}_2\text{O}$ , Htba<sup>−</sup>) and a change of the Htba<sup>−</sup> coordination. These factors induced higher distortion of the octahedra. It was assumed that hydrates, with a different number of coordinated water molecules, are more probable when the central metal has weaker bonds with O water molecules and with other ligands. The net topologies of **1–3** were compared. Thermal decomposition and IR spectra were analyzed for **1** and **2**.

## ARTICLE HISTORY

Received 12 April 2016  
Accepted 14 July 2016

## KEYWORDS


2-Thiobarbituric acid; Sodium; coordination compound; X-ray diffraction; infrared spectroscopy; thermal analysis



## 1. Introduction

In medicine, barbiturates are often used in the form of sodium salts, for example, sodium salt 5,5-diethylbarbituric acid (Veronal) and thiopental sodium. They are water-soluble and more readily absorbed than

**CONTACT** Maxim S. Molokeev  [msmolokeev@gmail.com](mailto:msmolokeev@gmail.com)

 Supplemental data for this article can be accessed here at <http://dx.doi.org/10.1080/00958972.2016.1228914>.

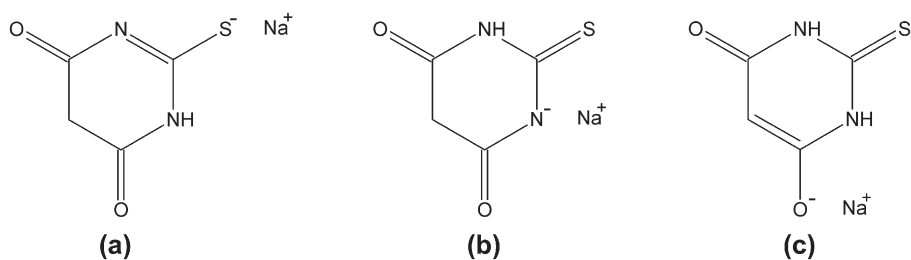


**Figure 1.** The probable schematic formulas of sodium 2-thiobarbiturate.

their parent compounds. 2-Thiobarbituric acid ( $H_2tba$ ) is a key compound of the group of medicines called thiobarbiturates. The related compound, for example, thiopental sodium is used as an anesthetic, anticonvulsant, and hypnotic medicine [1].  $H_2tba$  is used as the starting material in the synthesis of several derivatives which possess potentially useful biological activities [2, 3]. Due to the poor solubility in water and in most organic solvents,  $H_2tba$  is usually neutralized by sodium hydroxide to obtain a solution, but the use of the solid sodium salt of 2-thiobarbituric acid is preferable. There is the contradictory information about the crystal structure of this salt [4, 5]. Earlier, different structures were attributed to the commercially available sodium salt of  $H_2tba$ ,  $C_4H_3N_2NaO_2S$  (CAS No: 31645-12-2), as shown in figure 1(a) (Nowa Pharm. Co., Ltd., China; Alz Chem AG) and figure 1(b) (ICI Chem. Pvt. Ltd., India; Sigma-Aldrich). Besides, the thiomonocarbonyl form II (enol form) of  $H_2tba$  [6] is also stable, and therefore, the third variant of the sodium thiobarbiturate structure could be considered, as shown in figure 1(c).

It is interesting to find out how common this type of  $Htba^-$  coordination mode is for  $Na^+$  ions in **1** and **2**. As a rule, only one crystalline form of the barbiturate metal complex was obtained [7]. However, depending on the conditions of crystallization from solutions, a compound can be obtained in crystalline forms different in the nature or stoichiometry of included water molecules [8], the so-called hydrates. This subject has not been treated systematically though it is perceived to be of general importance, for example in the pharmaceutical industry. Early studies showed the formation of 2-thiobarbiturate hydrates of alkaline earth metals at different crystallization temperatures [9–11]. It can be reasonably assumed that the hydrates of sodium thiobarbiturate compounds are also common.

$H_2tba$  can be used as a building block to construct supramolecular assemblies with distinctive properties. The pronounced coordination properties combined to the possibility of non-covalent interactions ensure rich supramolecular chemistry of  $H_2tba$  complexes. The donor-acceptor features of  $H_2tba$  are important for crystal design of pharmaceuticals, molecular recognition, and catalytic activity [12]. The fundamental aim of the present study is to trace the changes in the solid-state sodium thiobarbiturate structures, as induced by the crystallization temperature variation in an aqueous medium.

## 2. Experimental

### 2.1. Reagents and synthesis

2-Thiobarbituric acid [CAS 504-17-6] with purity of >98% and 95% ethanol [CAS 64-17-5] was commercially available from Fluka. NaOH was obtained from Acros and used without purification.

0.2 g (1.4 mmole) of  $H_2tba$  acid was mixed with 2 mL of water and further with 0.056 g (1.4 mmole) of NaOH. A transparent light-yellow solution was obtained. The continuous water evaporation to volume ~0.5 mL from the hot solution at 60 °C resulted in the crystallization of almost colorless (with pink tint) precipitate. It was extracted from the hot solution and dried at room temperature between sheets of filter paper until constant weight. The mass of extracted precipitate of  $Na_2(H_2O)_3(Htba)_2$  (**1**) was 0.13 g, 49% yield. The higher solid product yield (about 90%) was reached during crystallization from the hot ethanol-based solution (95%). The single crystal of **1** was selected from the precipitate extracted from the hot ethanol-based solution.  $Na_2(H_2O)_4(Htba)_2$  (**2**) was crystallized from a water solution using the same starting reagents and

the solution composition. However, in this case, the solution saturated at 60 °C was quenched to 2–3 °C and filtered at this temperature. The precipitate was dried at room temperature to constant mass. Herewith, a colorless crystalline precipitate was obtained. The solid product yield was about 30% in reference to the initial H<sub>2</sub>tba. The residual concentrated filtrate was slowly evaporated at 2–3 °C to provide single crystals of **2**. However, we could not get a sufficient amount of the single-phase compound [Na<sub>2</sub>(H<sub>2</sub>O)<sub>5</sub>(Htba)<sub>2</sub>] (**3**), whose single crystals were earlier picked from the mixture of different phases [5].

The most stable phase in water solution is phase **1**. The products obtained from water solution always contain phase **1**, but, at room temperature, the impurities of **2** and **3** are also crystallized. Grinding of **1** in the presence of water does not lead to phase transformation (figure 8S). Storage at room temperature in the air during two weeks did not lead to transformation of **1** and **2** phases. Grinding of equimolar mixture of thiobarbituric acid with Na<sub>2</sub>CO<sub>3</sub> during 20 min led to formation of the new phase (or several new phases), and indexing of its powder pattern was unsuccessful. It was found that final product did not contain phases **1**, **2**, or **3**.

## 2.2. X-ray diffraction analysis

The intensity patterns were collected from single crystals of **1** and **2** at 25 °C using the D8 Venture X-ray single crystal diffractometer (Bruker AXS) equipped with a CCD-detector, graphite monochromator and Mo K $\alpha$  radiation source. Absorption corrections were applied using SADABS. The structures were solved by direct methods using SHELXS and refined in the anisotropic approach for non-hydrogen atoms using SHELXL [13]. All hydrogens of Htba<sup>-</sup> ligands in **1** and **2** were positioned geometrically as riding on their parent atoms with  $d(\text{C-H}) = 0.93 \text{ \AA}$  for the C5–H5 bond and  $d(\text{N-H}) = 0.86 \text{ \AA}$  for N–H bonds and  $U_{\text{iso}}(\text{H}) = 1.2 U_{\text{eq}}(\text{C,N})$ . All hydrogens of the H<sub>2</sub>O molecules were found via Fourier difference maps and refined without any geometrical restraints and  $U_{\text{iso}}(\text{H}) = 1.5 U_{\text{eq}}(\text{O})$ . The structural tests for the presence of missing symmetry elements and possible voids were produced using the PLATON program [14]. DIAMOND was used for crystal structure plotting [15].

The powder X-ray diffraction data were obtained using D8 ADVANCE (Bruker) diffractometer equipped by a VANTEC detector with a Ni filter. The measurements were made using Cu K $\alpha$  radiation. The structural parameters defined by single crystal analysis were used as a base in powder pattern Rietveld refinement. The refinement was performed using TOPAS 4.2. [16]. The low *R*-factors and good refinement results shown in figures 1S and 2S indicate the crystal structures of the powder samples to be representative ones of the **1** and **2** bulk structures.

## 2.3. Physical measurements

TGA was carried out on the simultaneous SDT-Q600 thermal analyzer (TA Instruments, USA) under dynamic air atmosphere (30 mL min<sup>-1</sup> flow rate) within 25–800 °C at the scan rate of 10 °C min<sup>-1</sup>. The qualitative composition of the evolved gasses was determined by FT-IR spectrometer Nicolet380 (Thermo Scientific, USA) combined with a thermal analyzer and with the TGA/FT-IR interface (attachment for the gas phase analysis). This setup allows simultaneous accumulation of the DTA and TG data and determining the composition of the released gas phase. The compound weight was 5.380 mg for **1** and 5.544 mg for **2**. Platinum crucibles with perforated lids were used. The IR absorption spectra of the compounds in KBr were recorded from 400–4000 cm<sup>-1</sup> at room temperature on a FT-IR spectrometer Nicolet 6700 (Thermo Scientific, USA, SFU CEJU).

## 3. Results and discussion

### 3.1. Crystal structures

The main structural characteristics of **1** and **2** are shown in table 1 and bond lengths are shown in table 1S. The Na–O and Na–S bond distances range from 2.311(1) to 2.442(4) Å and from 3.0833(6) to

**Table 1.** Crystal structure parameters of **1** and **2**.

Single crystal	Na(H <sub>2</sub> O) <sub>3</sub> (Htba) <sub>2</sub> ( <b>1</b> )	Na(H <sub>2</sub> O) <sub>4</sub> (Htba) <sub>2</sub> ( <b>2</b> )
Formula sum	C <sub>8</sub> H <sub>12</sub> N <sub>4</sub> Na <sub>2</sub> O <sub>7</sub> S <sub>2</sub>	C <sub>8</sub> H <sub>14</sub> N <sub>4</sub> Na <sub>2</sub> O <sub>8</sub> S <sub>2</sub>
Dimension (mm)	0.45 × 0.2 × 0.13	0.35 × 0.24 × 0.03
Color	Colorless	Colorless
Molecular weight	386.32	404.33
Temperature (K)	298	298
Space group, <i>Z</i>	<i>P</i> 2 <sub>1</sub> / <i>c</i> , 4	<i>P</i> 2 <sub>1</sub> 2 <sub>1</sub> 2, 4
<i>a</i> (Å)	10.418(1)	6.7075(6)
<i>b</i> (Å)	10.9492(8)	11.045(1)
<i>c</i> (Å)	13.682(1)	20.487(2)
$\beta$ (°)	110.206(2)	–
<i>V</i> (Å <sup>3</sup> )	1464.6(2)	1517.7(2)
$\rho_{\text{Calcd}}$ (g cm <sup>-3</sup> )	1.752	1.769
$\mu$ (mm <sup>-1</sup> )	0.465	0.457
Reflections measured	95,775	16,015
Reflections independent	4311	4439
Reflections with $F > 4\sigma(F)$	3813	3137
$2\theta_{\text{max}}$ (°)	60.36	60.11
<i>h, k, l</i> - limits	–14 ≤ <i>h</i> ≤ 14 –15 ≤ <i>k</i> ≤ 5; –19 ≤ <i>l</i> ≤ 9	–8 ≤ <i>h</i> ≤ 9 –15 ≤ <i>k</i> ≤ 4; –28 ≤ <i>l</i> ≤ 28
<i>R</i> <sub>int</sub>	0.0575	0.1019
Weighed refinement of <i>F</i> <sup>2</sup>	$w = 1/[\sigma^2(F_o^2) + (0.0356P)^2 + 0.8702P]$	$w = 1/[\sigma^2(F_o^2) + (0.0625P)^2 + 0.8355P]$
No. of refinement parameters	226	241
No. of restraints	6	8
<i>R</i> <sub>1</sub> [ <i>F</i> <sub>o</sub> > 4σ( <i>F</i> <sub>o</sub> )]	0.0263	0.0592
<i>wR</i> <sub>2</sub>	0.0690	0.1091
<i>Goof</i>	1.051	0.917
$\Delta\rho_{\text{max}}$ (e Å <sup>-3</sup> )	0.476	0.748
$\Delta\rho_{\text{min}}$ (e Å <sup>-3</sup> )	–0.372	–0.434
( $\Delta/\sigma$ ) <sub>max</sub>	0.001	0.001

3.264(2) Å, respectively. The distances are comparable to the values reported earlier for Na–O and Na–S bonds in six-coordinate **3** [5] and Na<sub>2</sub>(H<sub>2</sub>O)<sub>2</sub>Cl(Htba) (**4**) [4].

The asymmetric unit of the [Na<sub>2</sub>(H<sub>2</sub>O)<sub>*x*</sub>(Htba)<sub>2</sub>]<sub>*x*</sub> (*x* = 3, 4) unit cells contains two Na<sup>+</sup> ions, two Htba<sup>–</sup> ions and three and four H<sub>2</sub>O molecules, respectively (figures 2 and 3). Structures **1** and **2** are not isostructural, but the schemes show some similarity (figure 3(a,b)). The main difference is that the S atom is coordinated to two Na<sup>+</sup> ions in **1** forming a bridge (figures 2(a) and 3(a)), but, in **2**, the S is coordinated to only one Na<sup>+</sup> ion and the second Na<sup>+</sup> ion is coordinated to additional (fourth) H<sub>2</sub>O instead of the S (figures 2(b) and 3(b)). The previously reported compounds **3** and **4** also have the schemes (figure 3(c,d)) which are, to some extent, similar to those of **1** and **2** (figures 2(b) and 3(b)). The scheme of **3** is the most similar to that of **1** because both of them have the bridge S between two Na<sup>+</sup> ions. However, **3** has only one bridge H<sub>2</sub>O molecule instead of three bridge molecules in **1**. Na<sub>2</sub>(H<sub>2</sub>O)<sub>2</sub>Cl(Htba) has two H<sub>2</sub>O bridge molecules that relate this compound to other Na compounds with three (**1**), three (**2**), and one (**3**) bridging H<sub>2</sub>O molecules. The Cl<sup>–</sup> bridge and O bridge, however, noticeably estrange this compound from **1** to **3**.

In **1**, each Na<sup>+</sup> is coordinated by three H<sub>2</sub>O, two S, and one O of Htba<sup>–</sup> in an octahedron. Similarly, in **2**, the first Na<sup>+</sup> is coordinated by three H<sub>2</sub>O, two S, one O of Htba<sup>–</sup> in an octahedron. However, the second Na<sup>+</sup> is coordinated by four H<sub>2</sub>O, one S, one O of Htba<sup>–</sup> in an octahedron. The octahedra NaO<sub>4</sub>S<sub>2</sub> in **1** are connected directly through the SO<sub>2</sub> faces forming *r*(4) rings, and S, O nodes forming layers in the *bc* plane (figure 4(a)) with two ring motifs *r*(8) and *r*(16). The layers are joined through Htba<sup>–</sup> bridges forming a 3D net (figure 4(b)). The octahedra Na1O<sub>4</sub>S<sub>2</sub> and Na2O<sub>5</sub>S in **2** are connected directly through the SO<sub>2</sub> faces forming *r*(4) rings, and S, O nodes, forming a rod along the *a*-axis (figure 4(c)). These rods are joined through the Htba<sup>–</sup> bridge ions, forming a 3D net (figure 4(d)). Therefore, the main difference between **1** and **2** is the octahedral layers and rods, respectively. The reason for this transformation in **2** is that Na<sub>2</sub> lost one bridge S in its coordination sphere and it is replaced by the terminal H<sub>2</sub>O, which

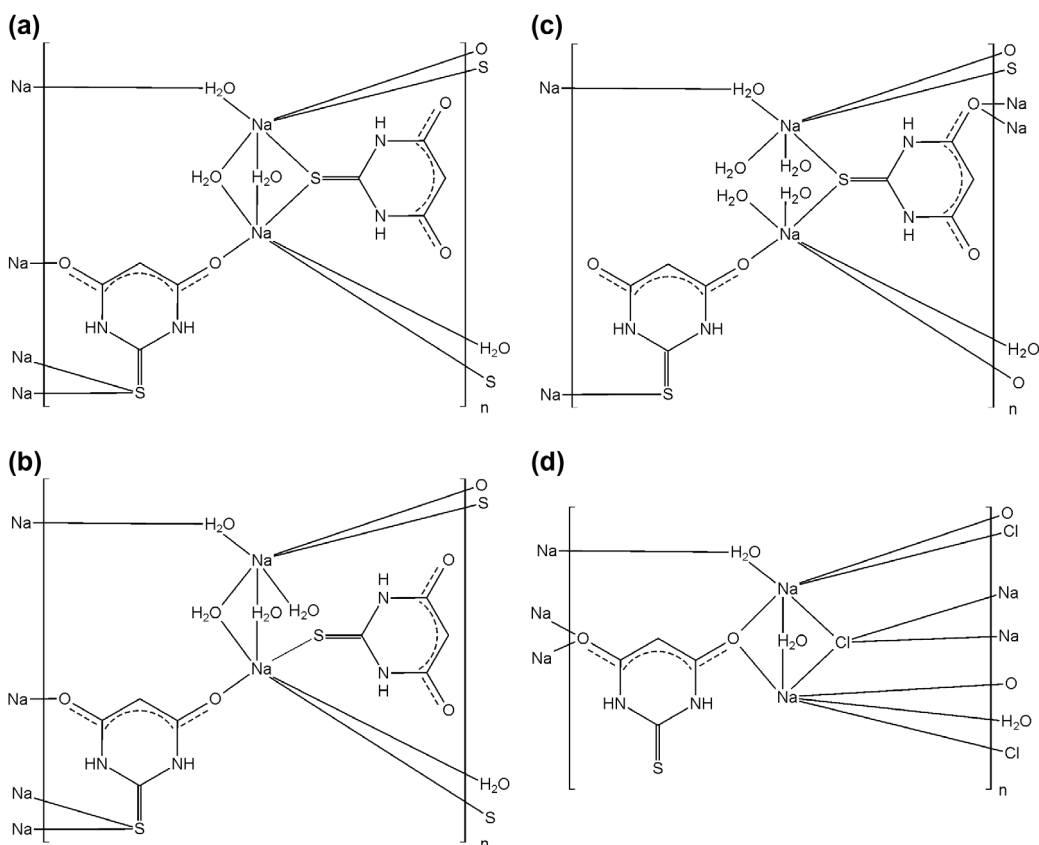


**Figure 2.** Schemes of  $\text{Na}_2(\text{H}_2\text{O})_x(\text{Htba})_2$ : (a)  $x = 3$  (**1**); (b)  $x = 4$  (**2**); (c)  $x = 5$  (**3**) and (d)  $\text{Na}_2\text{Cl}(\text{Htba})(\text{H}_2\text{O})_2$  (**4**). High-level similarity can be observed for schemes (a) **1** and (b) **2**. Scheme (c) violates similarity due to several  $\text{H}_2\text{O}$  molecules no longer participate in bridge bonding. Scheme (d) also shows discrepancy with other schemes, however, it has  $\dots\text{Na}-\text{H}_2\text{O}-\text{Na}-\text{H}_2\text{O}-\text{Na}\dots$  bridge like in (a) and (b).

is the fourth water molecule in **2**. This replacement of the S by terminal  $\text{H}_2\text{O}$  in the  $\text{Na}_2$  coordination sphere leads to change in supramolecular structure. There are 10 intermolecular hydrogen bonds in **1**, six  $\text{O}-\text{H}\cdots\text{O}$ , two  $\text{N}-\text{H}\cdots\text{O}$  and two  $\text{N}-\text{H}\cdots\text{S}$  which form the 3D net in which the pronounced 2D layers of  $\text{Htba}^-$  ions can be found in the  $ab$  plane (figure 5(a), table 2). These layers alternate with the layers of  $\text{Na}^+$  ions (figure 5(b)). All hydrogens of water molecules are involved in bonding with the formation of structural motifs  $\text{S}(6)$ ,  $\text{S}(10)$ ,  $\text{R}_2^1(6)$ ,  $\text{R}_2^1(8)$ ,  $\text{R}_2^2(8)$ ,  $\text{R}_3^3(12)$ ,  $\text{C}(8)$ ,  $\text{C}_3^3(16)$  (figure 5(a,b)). Contrary to that, there are 12 intermolecular hydrogen bonds in **2**, eight  $\text{O}-\text{H}\cdots\text{O}$ , two  $\text{N}-\text{H}\cdots\text{O}$  and two  $\text{N}-\text{H}\cdots\text{S}$ . They form the 3D net in which the pronounced 2D layers of  $\text{Htba}^-$  ions can be selected in the  $bc$  plane similar to those in **1** (figure 5(c), table 2). Just as in **1**, in **2**, these layers alternate with the  $\text{Na}^+$  ion layers (figure 5(d)). All hydrogens of water molecules in **2** are involved in bonding with the formation of structural motifs  $\text{S}(6)$ ,  $\text{R}_2^1(8)$ ,  $\text{R}_2^1(12)$ ,  $\text{R}_2^2(8)$ ,  $\text{R}_3^3(12)$ ,  $\text{C}(8)$  (figure 5(c,d)). The main difference between the supramolecular structures of **1** and **2** are due to the change of  $\text{S}(10)$  (**1**) to  $\text{R}_2^1(12)$  (**2**) and the transformation of  $\text{C}_3^3(16)$  in **1** to the chain of 12 atoms in **2**. H-bonds in **1** and **2** structures form the two same homosynths  $\text{R}_2^2(8)$ , and also other similar heterosynths  $\text{S}(6)$ ,  $\text{R}_2^1(8)$ ,  $\text{R}_3^3(12)$ ,  $\text{C}(8)$ . However, **2**, contrary to **1**, contains hydrogen bonds between water molecules (figure 5(a,c) and table 2). The H-bond patterns of **3** (figure 3S(a,b) and **4** (figure 3S(c,d) also showed the layered structure with  $\text{Htba}^-$  layers alternating with the layers of  $\text{Na}^+$  ions, but the periods of H-bond chain between the layers in all these compounds are different:  $\text{C}_3^3(16)$  in **1**; chain of 12 in (**2**);  $\text{C}(8)$  in **2**, **3** and  $\text{C}_2^1(12)$  in **4**. Compounds **1–4** form supramolecular motifs  $\text{S}(6)$  and  $\text{R}_2^2(8)$ .

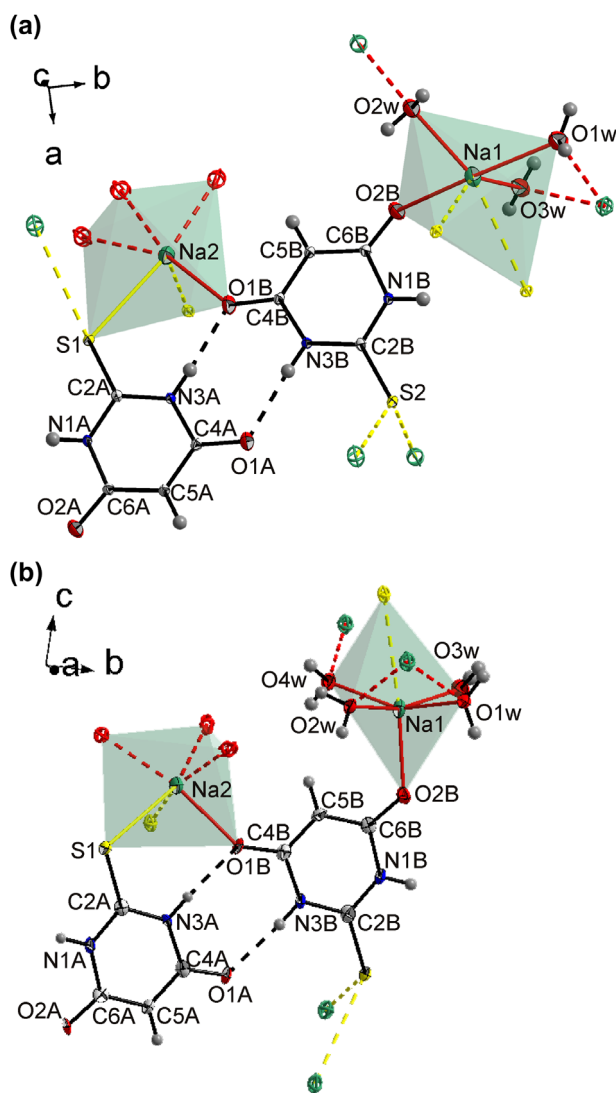


**Figure 3.** The asymmetric unit of the  $[\text{Na}_2(\text{H}_2\text{O})_x(\text{Htba})_2]$  unit cell: (a)  $x=3$  (**1**); (b)  $x=4$  (**2**). All atoms in the asymmetric unit are labeled. The directly neighboring symmetry-generated atoms are represented by principal ellipsoids with an individual color. The bonds linking asymmetric unit atoms with the symmetry-generated atoms and intermolecular hydrogen bonds are represented by dashed lines. The ellipsoids are drawn at the 50% probability level, except for the hydrogen atoms represented by spheres.

Head-to-head type  $\pi$ - $\pi$  interactions between the  $\text{Htba}^-$  rings are revealed in **1** and **2** by structural analysis (figure 4S, table 2S) using PLATON [14]. The bond lengths C2-S in **1** and **2** are 1.696–1.685 Å (table 1S), comparable to those reported for the C=S double bond (1.639(9) Å) in thiobarbiturate compounds. However, they are noticeably shorter than the theoretical value of a C-S single bond (1.78 Å). A slightly bigger value of the C2-S bond length, in comparison with that of the double C=S bond, can be explained by the coordination of  $\text{Htba}^-$  through S and the involvement of S in the H-bonds. Compounds **1** and **2** have very similar bond lengths O1-C4, O2-C6 and C4-C5, C5-C6 (table 1S) and that indicate the charge delocalization in the O=C-CH-C=O group. Such delocalization was previously observed in alkali and other metal compounds of 2-thiobarbiturates [4, 5, 9–11, 17–23] and 1,3-diethyl-2-thiobarbiturates [24–27].

The polyhedral distortion calculated using the equation  $D = (1/n)\sum((L_i - L_{av})/L_{av})$ , where  $L_i$  is the distance from the central atom to the  $i^{\text{th}}$  coordinating atom and  $L_{av}$  is the average bond length [28], showed



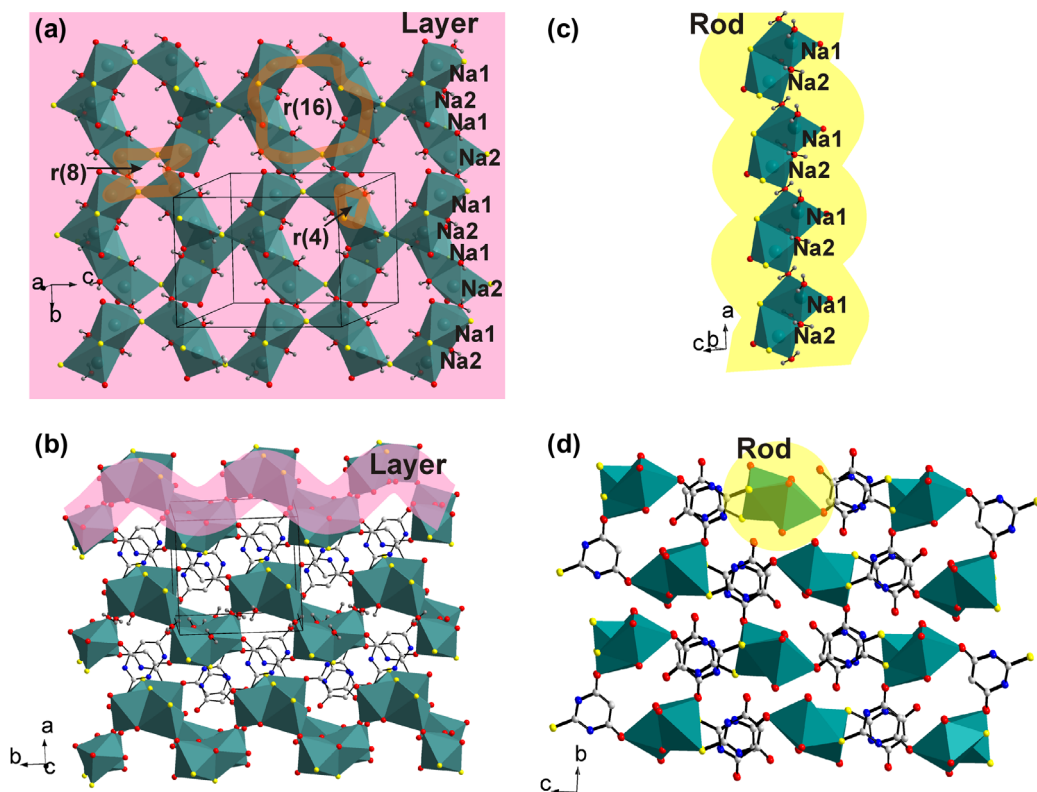


**Figure 4.** The layer formed by  $\text{NaO}_5\text{S}_2$  octahedra in the *bc* plane of **1** (a), and the rod formed by  $\text{Na}_1\text{O}_5\text{S}_2$  and  $\text{Na}_2\text{O}_5\text{S}$  octahedra along the *a*-axis of **2** (c), all Htba<sup>-</sup> ions are omitted for clarity. The 3-D network of octahedra layers/rods linked with each other by bridging Htba<sup>-</sup> ions (b) in **1** and (d) in **2**, all hydrogens and terminal Htba<sup>-</sup> ions are omitted for clarity.

decreasing values with the increasing *x* from 3 to 5 for  $[\text{Na}_2(\text{H}_2\text{O})_x(\text{Htba})_2]$  (table 1S). The increase of the number of terminal water molecules in the structures is accompanied by reduction of the strained 4-membered rings, which are formed by two bridging water molecules and two Na(I) ions, along with a change in the local surrounding Na<sup>+</sup> ions and this reduces the geometric distortion of the coordination polyhedra.

Hydrates are molecules obtained in crystalline forms that differ in the nature or the stoichiometry of included water molecules [8]. Therefore, **1–3** can be considered as hydrates, like earlier characterized compounds:  $[\text{Ba}(\text{H}_2\text{O})_2(\mu_3\text{-Htba-O,S,S})_2]_n$  and  $[\text{Ba}(\mu_2\text{-H}_2\text{O})(\text{H}_2\text{O})_2(\mu_4\text{-Htba-O,O',S})(\text{Htba-O})]_n \cdot 2n\text{H}_2\text{O}$  [10];  $[\text{Sr}(\mu_2\text{-H}_2\text{O})_2(\text{H}_2\text{O})_2(\mu_2\text{-Htba-O,O})(\text{Htba-O})]_n \cdot n\text{H}_2\text{O}$  [11] and  $[\text{Sr}(\text{H}_2\text{O})_4(\mu_2\text{-Htba-O,S})_2]_n$  [9];  $\text{Ca}_2(\text{H}_2\text{O})_8(\mu_2\text{-Htba-O,O'})_2(\text{Htba-O})_2$  and  $[\text{Ca}(\text{H}_2\text{O})_5(\text{Htba-O})_2] \cdot 2\text{H}_2\text{O}$  [9]. Thus, it can be assumed that hydrates, from formation of several phases of the same compound with a different content of coordinated water, is common for alkali and alkaline earth ions. This can be attributed, at least partly, to the relatively low value of the binding energy M–O<sub>w</sub> of the s-metal ions which facilitates the mutual transitions in hydrates.

### 3.2. Topological analysis of **1** and **2**

The topological analysis of the 3D-networks in **1** and **2** was implemented using the representation of Htba<sup>-</sup> and H<sub>2</sub>O molecules as the spheres which were located in their centroids. The ToposPro program was used to make the structure simplification by the standard method [29] and, after the procedure, the 0,1,2-coordinated nodes were omitted. The obtained networks were used to calculate the topological indices in ToposPro [29], which were further used to identify the nets and assignment to the s topological type.



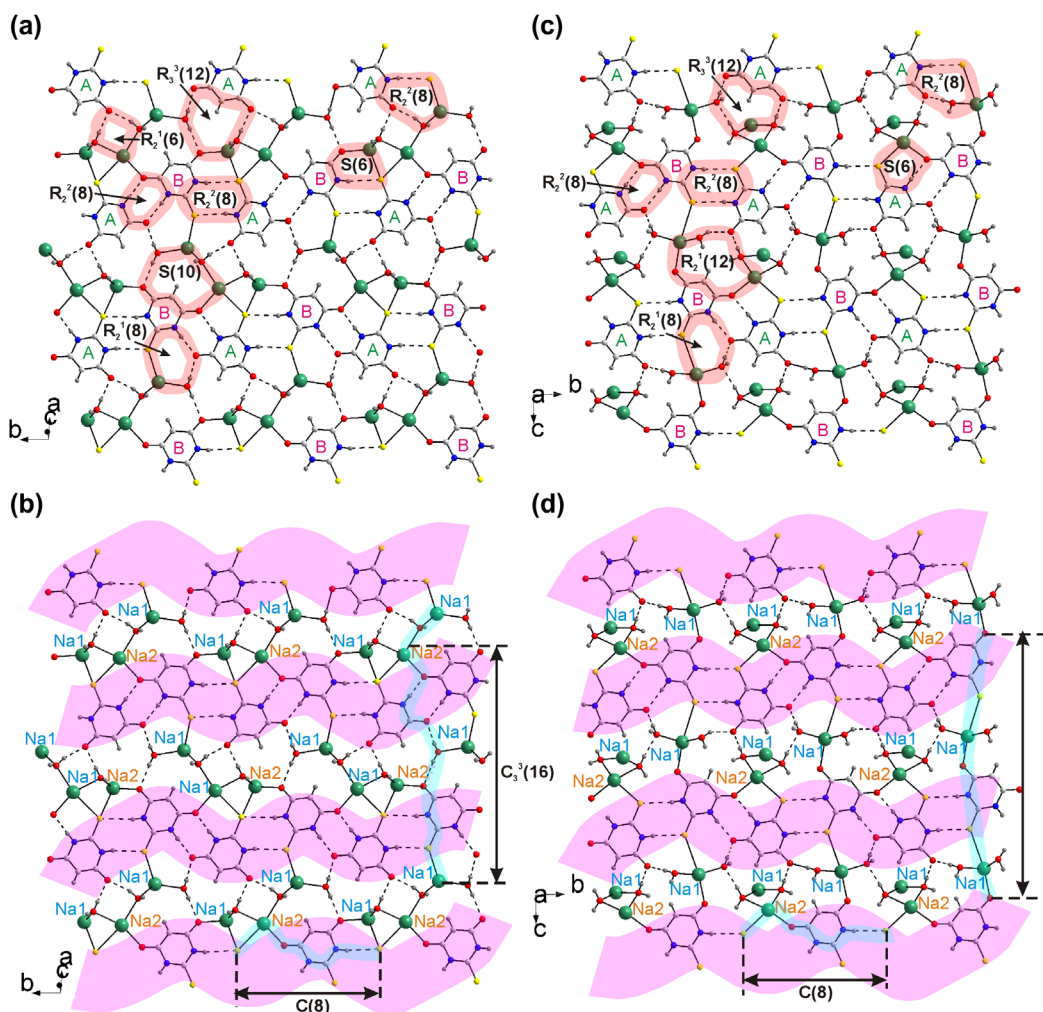


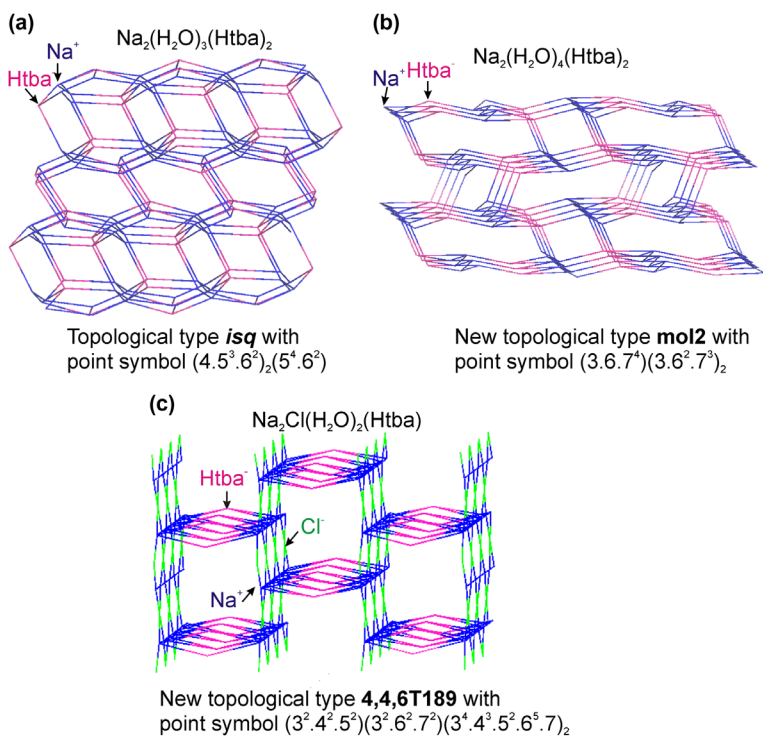
**Figure 5.** Hydrogen bonding in **1** (a, b) and **2** (c, d). The H-bonds are marked by dashed lines, the H-bond motifs are marked by circles and broad lines. A and B indicate independent  $\text{Htba}^-$  ions.

In **1**, the  $\text{Na1}^+$  and  $\text{Na2}^+$  ions are linked by three  $\text{Htba}^-$  ligands and three  $\text{H}_2\text{O}$  bridge molecules; one  $\text{Htba}^-$  ligand bridges two  $\text{Na}^+$  ions and the other  $\text{Htba}^-$  ligand bridges four  $\text{Na}^+$  ions. The simplification and omitting of the 0,1,2-coordinated nodes leave only three nodes: the ( $\text{Na1}^+$ ) node coordinated by two ( $\text{Na2}^+$ ) nodes and two ( $\text{Htba}^-$ ) nodes; the ( $\text{Na2}^+$ ) node coordinated by two ( $\text{Na1}^+$ ) nodes and two ( $\text{Htba}^-$ ) nodes; the ( $\text{Htba}^-$ ) node coordinated by two ( $\text{Na1}^+$ ) nodes and two ( $\text{Na2}^+$ ) nodes. It should be noted that the ( $\text{Htba}^-$ ) node has the same point symbol as the ( $\text{Na1}^+$ ) node –  $(4.5^3.6^2)$ . Although the two nodes are chemically different, in our case the two nodes are topologically equivalent and, consequently, **1** has the binodal (4,4)-connected 3D-net with the point symbol  $(4.5^3.6^2)_2(5^4.6^2)$  which is known as the **isq** net (figure 6(a)).

In **2**, the  $\text{Na2}^+$ , like that in **1**, is linked by three  $\text{Htba}^-$  ligands and three  $\text{H}_2\text{O}$  bridge molecules. However, the  $\text{Na1}^+$  ion is linked by two  $\text{Htba}^-$  ligands and four  $\text{H}_2\text{O}$  bridge molecules; one  $\text{Htba}^-$  ligand bridges one  $\text{Na}^+$  ion and the other  $\text{Htba}^-$  ligand bridges four  $\text{Na}^+$  ions. The simplification and omitting of the 0,1,2-coordinated nodes leave only three nodes like in **1**: the ( $\text{Na1}^+$ ) node coordinated by two ( $\text{Na2}^+$ ) nodes and two ( $\text{Htba}^-$ ) nodes; the ( $\text{Na2}^+$ ) node coordinated by two ( $\text{Na1}^+$ ) nodes and two ( $\text{Htba}^-$ ) nodes; the ( $\text{Htba}^-$ ) node coordinated by two ( $\text{Na1}^+$ ) nodes and two ( $\text{Na2}^+$ ) nodes. In spite of this similarity, the

**Table 2.** Hydrogen-bond geometry in **1** and **2** (Å, °).

D–H	d(D–H)	d(H···A)	∠D–H···A	D···A	A	Transformation for A atom
<b>Na(H<sub>2</sub>O)<sub>3</sub>(Htba)<sub>2</sub> (1)</b>						
N1A–H1A	0.86	2.44	169	3.288(1)	S2	$x, -1 + y, z$
N1B–H1B	0.86	2.55	171	3.406(1)	S1	$x, 1 + y, z$
N3A–H3A	0.86	1.89	176	2.744(1)	O1B	$x, y, z$
N3B–H3B	0.86	2.01	166	2.848(1)	O1A	$x, y, z$
O1W–H11	0.86(2)	2.06(2)	167(2)	2.899(1)	O2B	$-x, 1/2 + y, 1/2 - z$
O1W–H12	0.87(2)	1.96(2)	163(2)	2.803(1)	O1A	$1 - x, 2 - y, 1 - z$
O2W–H21	0.84(2)	2.01(2)	158(2)	2.802(1)	O2A	$1 - x, 1 - y, 1 - z$
O2W–H22	0.80(2)	1.98(2)	175(2)	2.780(1)	O2A	$-1 + x, 1 + y, z$
O3W–H31	0.83(2)	2.07(2)	171(2)	2.895(1)	O1A	$1 - x, 1/2 + y, 1/2 - z$
O3W–H32	0.84(2)	1.86(2)	177(2)	2.701(1)	O2A	$-1 + x, 3/2 - y, -1/2 + z$
<b>Na(H<sub>2</sub>O)<sub>4</sub>(Htba)<sub>2</sub> (2)</b>						
N1A–H1A	0.86	2.47	170	3.315(5)	S2	$x, -1 + y, z$
N1B–H1B	0.86	2.46	172	3.316(4)	S1	$x, 1 + y, z$
N3A–H3A	0.86	1.96	177	2.814(5)	O1B	$x, y, z$
N3B–H3B	0.86	1.99	174	2.843(5)	O1A	$x, y, z$
O1W–H11	0.89(5)	1.93(5)	165(5)	2.802(5)	O3 W	$1/2 + x, 3/2 - y, 2 - z$
O1W–H12	0.89(5)	2.05(5)	155(5)	2.876(5)	O1A	$3/2 - x, 1 - y, 1/2 + z$
O2W–H21	0.87(5)	1.88(5)	167(5)	2.733(5)	O2A	$3/2 - x, -y, 1/2 + z$
O2W–H22	0.87(4)	1.93(5)	174(4)	2.801(5)	O2A	$2 - x, 1/2 + y, 3/2 - z$
O3W–H31	0.85(5)	2.14(5)	155(5)	2.826(5)	O2B	$-1/2 + x, 3/2 - y, 2 - z$
O3W–H32	0.87(5)	1.90(4)	170(5)	2.758(5)	O1A	$3/2 - x, 1 - y, 1/2 + z$
O4W–H41	0.84(5)	2.29(5)	147(4)	3.029(5)	O2A	$3/2 - x, -y, 1/2 + z$
O4W–H42	0.87(4)	2.00(5)	173(6)	2.864(5)	O2A	$1 - x, 1/2 + y, 3/2 - z$


**Figure 6.** A schematic representation of the network topologies of (a) **1**, (b) **2**, and (c) **4**.

(Na1<sup>+</sup>) and (Na2<sup>+</sup>) nodes in **2** have the same point symbol – (3.6<sup>2</sup>.7<sup>3</sup>), but the (Htba<sup>-</sup>) node has another point symbol – (3.6.7<sup>4</sup>). As far as the two Na nodes are chemically and topologically equivalent, consequently, **2** has the binodal (4,4)-connected 3D-net with the point symbol (3.6.7<sup>4</sup>)(3.6<sup>2</sup>.7<sup>3</sup>)<sub>2</sub> (figure 6(b)) which is a new topological net is added to the ToposPro database [29] and named **mol2** net.

The topological analysis of **3** revealed that it forms a 1D-chain and, therefore, the point symbol cannot be obtained. However, the topological analysis of **4** showed a 3-nodal (4,4,6) 3D network with point symbol (3<sup>2</sup>.4<sup>2</sup>.5<sup>2</sup>)(3<sup>2</sup>.6<sup>2</sup>.7<sup>2</sup>)(3<sup>4</sup>.4<sup>3</sup>.5<sup>2</sup>.6<sup>5</sup>.7)<sub>2</sub> (figure 6(c)) which is also new topology and is added to the database as the **4,4,6T189** net. The diversity of the net topology found for coordination compounds of Htba<sup>-</sup> with Na<sup>+</sup> is intriguing and is promising for the search of exotic topological nets.

### 3.3. IR spectroscopy

The IR spectra of **1**, **2** and H<sub>2</sub>tba are markedly different from each other from 3500–3300 cm<sup>-1</sup> (figure 5S). In this range, the H<sub>2</sub>tba spectrum is without bands. The IR spectrum of **1** contains sharp bands at 3462, 3424, and 3349 cm<sup>-1</sup>, but the spectrum of **2** possesses the broad shoulder over the range of 3400–3300 cm<sup>-1</sup> associated with ν(O–H) of coordinated water molecules. In the range of ν(C–O) vibrations, intense bands of H<sub>2</sub>tba at 1708 and 1684 cm<sup>-1</sup> are shifted to a lower frequency to 1645 and 1628 cm<sup>-1</sup> (for **1**) and down to 1654 and 1614 cm<sup>-1</sup> (for **2**), which is consistent with coordination of the Htba<sup>-</sup> through oxygen. The characteristic band at 1142 cm<sup>-1</sup> that was previously assigned to ν(C=S) stretch [30] is absent in spectra of **1** and **2**, which means that the C=S group is involved in coordination with Na<sup>+</sup> ions.

### 3.4. Thermal decomposition

As can be seen from the IR spectroscopic analysis of released gasses, thermal decomposition of **1** starts at ~110 °C with loss of coordinated water molecules, accompanied by the endo effect at 116.6 °C (figure 6S). Starting from ~140 to ~350 °C, the sample mass is practically persistent, and the mass lost (Δ*m*) at 140 °C (13.6%) almost coincides with the value calculated assuming the release of three water molecules (13.99%). The oxidation of Htba<sup>-</sup> occurs at *T* > 350 °C and the sample mass rapidly decreases. According to the mean TG curve, the thermal decomposition occurs in three or more stages. At the first stage (~360–400 °C), the mass loss rate is maximal (Δ*m* = 29.2%) and the strong exothermal effect at 392.7 °C is associated with the process. The second (~400–520 °C) and, especially, third (~520–650 °C) stages show a much slower mass loss under cooling. The second stage of oxidative decomposition is accompanied by two exo effects at 457.0 and 503.6 °C. The IR data recorded during the decomposition of **1** showed a release of gaseous H<sub>2</sub>O, CO<sub>2</sub>, and SO<sub>2</sub>, as for other thiobarbituric coordination compounds [31]. In the temperature interval of ~650–700 °C, the mass is invariant. The total Δ*m* at 700 °C is equal to 71.1%. However, in terms of the formation of only Na<sub>2</sub>SO<sub>4</sub>, it should be less (63.23%). One can assume that, similarly to the thermal decomposition of thiobarbiturates with alkaline earth metals [9], **1** under oxidative conditions at 700 °C transforms to a mixture of Na<sub>2</sub>SO<sub>4</sub> and Na<sub>2</sub>O.

The decomposition of **2** also starts from dehydration at ~90 °C, which ends at ~150 °C (figure 7S), accompanied by the endo effect at 95.9 °C. Over the range of ~150–350 °C, the sample mass is constant, but Δ*m* at 150 °C (14.9%) does not coincide with the value calculated assuming the removal of all four coordinated water molecules (17.8%). This inconsistency can be explained by an impurity and partial dehydration during the sample storage in the air before thermal analysis. The water lost at 150 °C (see figures 6S and 7S) of **1** and **2** led to different final products because powder diffraction patterns are different. We tried our best but could not index these powder patterns, supposedly because they are multiphase mixtures. The obtained final products are hygroscopic and unstable under air. Similarly to the thermolysis of **1**, the oxidation of Htba<sup>-</sup> at *T* > 350 °C occurs in several stages (figure 7S). At the first stage (~360–450 °C), the mass loss rate is maximal (Δ*m* = 33.5%), and it corresponds to the strong endothermic effect at 416.7 °C. The other two stages are accompanied by the exo effects at 489.7 and 686.3 °C, respectively. In the temperature range of ~720–800 °C, the mass stays constant.

The thermolysis of **2**, similar to that of **1**, induces the release of gaseous  $\text{H}_2\text{O}$ ,  $\text{CO}_2$  and  $\text{SO}_2$ . The total  $\Delta m$  at  $700\text{ }^\circ\text{C}$  is 71.1%. In terms of the formation of only  $\text{Na}_2\text{SO}_4$ , it should be less (64.9%). Thus, it can be supposed that, like in the case of thermal decomposition of **1**, the oxidative decomposition of **2** at  $720\text{ }^\circ\text{C}$  leads to the  $\text{Na}_2\text{SO}_4$  and  $\text{Na}_2\text{O}$  mixture formation. The comparison of thermal decomposition of **1** and **2** show a similar character of TG and DSC curves, but the temperatures are different, for example, the dehydration of **2** starts  $\sim 20\text{ }^\circ\text{C}$  lower than that in **1**.

## 4. Conclusion

At least three polymeric hydrated forms of sodium thiobarbiturate of different composition and structure can be crystallized from solutions. Compound **1** with the smallest water content is well crystallized at  $60\text{ }^\circ\text{C}$  from water and water-alcohol solutions. Comparatively, **2** is precipitated from water solution under quenching. The crystals of **3**, which contain more water, are universally crystallized in combination with other phases, including **1** and **2**, under slow evaporation of a solution at room temperature [5].  $\text{Na}^+$  in **1–3** is octahedral, linked to  $\text{Htba}^-$  ions through O and S (figure 2); O,S-coordination of  $\text{H}_2\text{tba}$  was found in coordination compounds of thiobarbiturates with K ions [32, 33]. When boiling aqueous solution contains equimolar amounts of barbituric acid and cesium hydroxide, the unexpected product crystallizes, 5-hydroxyhydrurilic acid, which forms a coordination compound with Cs ion [34]. Probably, such reaction can undergo with  $\text{H}_2\text{tba}$ . The sequence of compounds **1–2–3**, ranked by the number of coordinated water molecules, showed a decreasing number of bridged water molecules, which form sterically strained 4-membered rings, and, in combination with the changes of ligand coordination of  $\text{Na}^+$ , this leads to a decrease of octahedral distortion. Sodium thiobarbiturates **1–3** with different coordinated water molecules are hydrates [8]. Earlier, hydrates were also obtained for thiobarbiturates of alkali earth metals [9–11]. It can be reasonably supposed that such form of hydrates is especially common for the metal ions which form relatively weak chemical bonds with coordinated water molecules and other ligands, and that leads to coexistence of different hydrate forms with a similar crystal lattice energy value. The diversity of the net topology found for the coordination compounds of  $\text{Htba}^-$  with  $\text{Na}^+$  is intriguing and it is very promising for a search of exotic topological nets. The dehydration of **1** and **2** starts at  $\sim 90$  and  $\sim 110\text{ }^\circ\text{C}$ , respectively. Further, at  $T > 350\text{ }^\circ\text{C}$ , thermal decomposition proceeds for several stages with the release of gaseous  $\text{H}_2\text{O}$ ,  $\text{CO}_2$ , and  $\text{SO}_2$ .

## Supplementary material

The crystallographic data for the structural analysis have been deposited with the Cambridge Crystallographic Data Center ((**1**) – CCDC # 1472785; (**2**) – CCDC # 1472786). The information may be obtained free from CCDC Director: 12 Union Road, Cambridge CB2 1EZ, UK (Fax: +44(1223)336–033, E-mail: [deposit@ccdc.cam.ac.uk](mailto:deposit@ccdc.cam.ac.uk), or [www.ccdc.cam.ac.uk](http://www.ccdc.cam.ac.uk)).

## Acknowledgements

The study was carried out within the public task of the Ministry of Education and Science of the Russian Federation for research engineering of the Siberian Federal University in 2016 (project no. 3049). V.V.A. is grateful to the Ministry of Education and Science of the Russian Federation for the financial support of the investigation. X-ray data from single crystals were obtained with use the analytical equipment of Baikal Center of collective use of SB RAS, X-ray data from powders were obtained with use the analytical equipment of Krasnoyarsk Center of collective use of SB RAS.

## Disclosure statement

No potential conflict of interest was reported by the authors.

## Funding

This work was supported by the the Ministry of Education and Science of the Russian Federation for research engineering of the Siberian Federal University [grant number 3049].

## References

- [1] L.S. Goodman, A. Gilman. *Pharmacological Basis of Therapeutics*, p. 98, The MacMillan Company, London (1970).
- [2] V.K. Ahluwalia, R. Aggarwal. *Proc. Ind. Nat. Sci. Acad.*, **5**, 369 (1996).
- [3] A.I. Rakhimov, S.A. Avdeev. Thi Doan Le Chang, *Russ. J. Gen. Chem.*, **79**, 338 (2009).
- [4] B. Li, W. Li, L. Ye, G.-F. Hou, L.-X. Wu. *Acta Cryst. E*, **66**, m1546 (2010).
- [5] N.N. Golovnev, M.S. Molokeev. *Acta Cryst. C*, **69**, 704 (2013).
- [6] M.R. Chierotti, L. Ferrero, N. Garino, R. Gobetto, L. Pellegrino, D. Braga, F. Grepioni, L. Mani. *Chem. Eur. J.*, **16**, 4347 (2010).
- [7] *Cambridge Structural Database, Version 5.36*, University of Cambridge, Cambridge, UK (2014).
- [8] A. Nangia, G.R. Desiraju. *Chem. Commun.*, **7**, 605 (1999).
- [9] N.N. Golovnev, M.S. Molokeev, S.N. Vereshchagin, V.V. Atuchin. *J. Coord. Chem.*, **66**, 4119 (2013).
- [10] N.N. Golovnev, M.S. Molokeev. *J. Struct. Chem.*, **55**, 912 (2014).
- [11] N.N. Golovnev, M.S. Molokeev. *Russ. J. Inorg. Chem.*, **59**, 72 (2014).
- [12] K.T. Mahmudov, M.N. Kopylovich, A.M. Maharramov, M.M. Kurbanova, A.V. Gurbanov, A.J.L. Pombeiro. *Coord. Chem. Rev.*, **265**, 1 (2014).
- [13] G.M. Sheldrick. *Acta Cryst A*, **64**, 112 (2008).
- [14] A.L. Spek. *J. Appl. Cryst.*, **36**, 7 (2003).
- [15] W.T. Pennington. *J. Appl. Cryst.*, **32**, 1028 (1999).
- [16] *Bruker AXS TOPAS V4: General profile and structure analysis software for powder diffraction data—User's Manual*, Bruker AXS, Karlsruhe, Germany (2008).
- [17] N.N. Golovnev, M.S. Molokeev. *Russ. J. Inorg. Chem.*, **58**, 1193 (2013).
- [18] N.N. Golovnev, M.S. Molokeev. *J. Struct. Chem.*, **54**, 968 (2013).
- [19] N.N. Golovnev, M.S. Molokeev, M.Y. Belash. *J. Struct. Chem.*, **54**, 566 (2013).
- [20] N.N. Golovnev, M.S. Molokeev. *J. Struct. Chem.*, **55**, 125 (2014).
- [21] N.N. Golovnev, M.S. Molokeev. *Russ. J. Inorg. Chem.*, **59**, 943 (2014).
- [22] N.N. Golovnev, M.S. Molokeev. *Russ. J. Coord. Chem.*, **40**, 648 (2014).
- [23] N.N. Golovnev, M.S. Molokeev, S.N. Vereshchagin, V.V. Atuchin. *J. Coord. Chem.*, **68**, 1865 (2015).
- [24] N.N. Golovnev, M.S. Molokeev, I.I. Golovneva. *Russ. J. Coord. Chem.*, **41**, 300 (2015).
- [25] N.N. Golovnev, M.S. Molokeev, M.A. Lutoshkin. *Russ. J. Inorg. Chem.*, **60**, 572 (2015).
- [26] N.N. Golovnev, M.S. Molokeev, S.N. Vereshchagin, I.V. Sterkhova, V.V. Atuchin. *Polyhedron*, **85**, 493 (2015).
- [27] M.S. Molokeev, N.N. Golovnev, S.N. Vereshchagin, V.V. Atuchin. *Polyhedron*, **98**, 113 (2015).
- [28] W. Baur. *Acta Cryst. B*, **30**, 1195 (1974).
- [29] V.A. Blatov, A.P. Shevchenko, D.M. Proserpio. *Cryst. Growth Des.*, **14**, 3576 (2014).
- [30] E. Mendez, M.F. Cerda, J.S. Gancheff, J. Torres, C. Kremer, J. Castiglioni, M. Kieninger, O.N. Ventura. *J. Phys. Chem. C*, **111**, 3369 (2007).
- [31] N.N. Golovnev, M.S. Molokeev, S.N. Vereshchagin, V.V. Atuchin, M.Y. Sidorenko, M.S. Dmitrushkov. *Polyhedron*, **70**, 71 (2014).
- [32] V.I. Balas, I.I. Verginadis, G.D. Geromichalos, N. Kourkoumelis, L. Male, M.B. Hursthouse, K.H. Repana, E. Yiannaki, K. Charalabopoulos, T. Bakas, S.K. Hadjidakou. *Eur. J. Med. Chem.*, **46**, 2835 (2011).
- [33] M. Kubicki, A. Owczarzak, V.I. Balas, S.K. Hadjidakou. *J. Coord. Chem.*, **65**, 1107 (2012).
- [34] G.S. Nichol, W. Clegg. *Acta Cryst.*, **C61**, m459 (2005).